

## Radiotracer and Thermal Desorption Studies of Dehydrogenation and Atmospheric Hydrogenation of Organic Fragments Obtained from [ $^{14}\text{C}$ ]Ethylene Chemisorbed over Pt(111) Surfaces

S. M. DAVIS,<sup>1</sup> F. ZAERA, B. E. GORDON, AND G. A. SOMORJAI

*Materials and Molecular Research and Chemical Biodynamics Divisions, Lawrence Berkeley Laboratory, and Department of Chemistry, University of California, Berkeley, Berkeley, California 94720*

Received July 16, 1984; revised November 21, 1984

The energetics and reversibility of ethylene sequential dehydrogenation on the (111) platinum single crystal surface has been investigated at 300–600 K using thermal desorption spectroscopy and a carbon-14 radiotracer technique. Ethylidyne species produced by [ $^{14}\text{C}$ ]C<sub>2</sub>H<sub>4</sub> chemisorption at 300–400 K were stable with respect to hydrogenation at room temperature. However, at atmospheric hydrogen pressure and temperatures above 350 K, ethylidyne species were easily eliminated from the platinum surface by hydrogenation. For [ $^{14}\text{C}$ ]C<sub>2</sub>H<sub>4</sub> adsorption temperatures above 450 K, radiotracer studies revealed the presence of both “active” and “inactive” forms of partially dehydrogenated carbonaceous deposits on the platinum surface which differ greatly in their reactivity for hydrogenation and hydrogen transfer with unlabeled hydrocarbons. The inactive fraction increased with increasing adsorption temperature as the surface species became more hydrogen deficient. Removal of the active  $^{14}\text{C}$ -containing species by hydrogen transfer occurred readily.

© 1985 Academic Press, Inc.

### INTRODUCTION

The formation of stable alkylidyne surface species with well-defined atomic structure has now been carefully demonstrated for the hexagonal (111) crystal faces of rhodium (1), palladium (2), and platinum (3–6). In the case of platinum, recent reaction studies in our laboratory (7) have provided direct evidence for an olefin hydrogenation mechanism wherein the alkylidyne surface species function as an important and unique co-catalyst in the hydrogenation pathway. Specifically, during ethylene hydrogenation at atmospheric pressures and 300–370 K, an ordered ethylidyne (Pt<sub>3</sub>≡CCH<sub>3</sub>) overlayer is formed immediately as the reaction commences. High-resolution electron energy loss spectroscopy (HREELS) (8) and a radiotracer technique (reported here), have

both shown that this ethylidyne is stable toward rehydrogenation and desorption under the conditions where ethylene hydrogenation occurs (300 K, 1 atm H<sub>2</sub>). Hydrogen–deuterium exchange of the methyl group in ethylidyne is also a slow process in comparison to the high-pressure hydrogenation (5, 7–9). It now appears very likely that the hydrogenation reaction actually takes place on top of this ordered metal–organic layer, which acts as a transfer agent for hydrogen atoms from the metallic surface to the reactant ethylene. Furthermore, it appears that the “structure insensitivity” of ethylene hydrogenation over platinum catalysts (10, 11), originates at least in part from the presence of this active ethylidyne layer which effectively masks the underlying platinum structure.

At higher temperatures (450–800 K), the chemistry of all hydrocarbons adsorbed on platinum is dominated by dissociative chemisorption involving the scission of one or more C–H bonds (12). Detailed under-

<sup>1</sup> Present address: Exxon Research and Development Laboratory, P.O. Box 2226, Baton Rouge, Louisiana 70821.

standing of these elementary C–H bond breaking processes is essential for establishing reaction mechanisms for important hydrocarbon skeletal rearrangements such as isomerization and aromatization. These reactions are catalyzed directly at metal sites (13, 14), and only at high temperatures ( $\geq 500$  K), where C–H bond breaking occurs easily. Of particular importance are the energetics and reversibility of the sequential C–H bond breaking processes.

Hydrogen thermal desorption (TDS) and carbon-14 radiotracer studies have been applied here to investigate the energetics and reversibility of ethylene sequential dehydrogenation on the flat (111) platinum single crystal surface. The evolution of hydrogen under UHV conditions was monitored as a function of adsorption temperature to determine the activation energies for sequential C–H bond breaking and the average (H/C) composition of the adsorbed species. Simultaneous radiotracer studies were employed to explore the adsorption reversibility. Reactivity studies carried out near atmospheric pressure revealed two distinct types of carbonaceous species on the platinum surfaces: (1) an active form consisting of ethylidyne species and fragments which undergo hydrogenation and hydrogen transfer under mild conditions, and (2) an inactive form that displays little reactivity over the entire range of temperature (300–700 K) and pressure ( $10^{-10}$ –1 atm) investigated.

Removal of the active  $^{14}\text{C}$ -containing species by hydrogen transfer reactions with unlabeled hydrocarbons was also studied, and significant reaction rates at 520–570 K for such processes were found. The proportion of the total surface carbon which exists in the active form decreased with increasing adsorption temperature as the surface species became more hydrogen deficient.

#### EXPERIMENTAL

Experiments were carried out in an ultrahigh vacuum (UHV) system, described previously (14), that was equipped with facili-

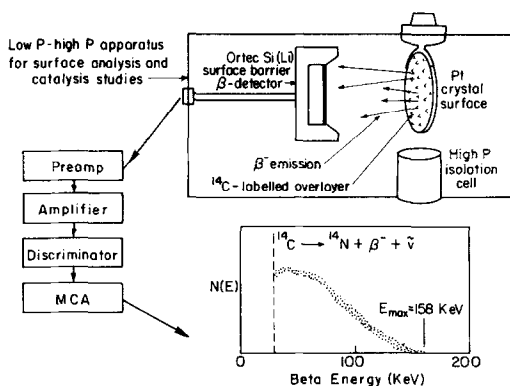


FIG. 1. Schematic diagram of the radiotracer counting system for adsorption and catalysis studies using small area surfaces in ultrahigh vacuum.

ties for low-energy electron diffraction, Auger electron spectroscopy, thermal desorption, radiotracer analysis, and *in situ* sample treatment at atmospheric pressures. The counting system for  $^{14}\text{C}$  radiotracer studies was detailed in a separate report (15), and is shown schematically in Fig. 1. It consisted of a solid-state surface barrier detector which was mounted on a rotative feedthrough in the center of the UHV chamber. The detector could be reproducibly positioned directly in front of the single crystal surface (within 1 cm) for counting adsorbed species, or rotated away for background corrections, high-pressure reactions, or LEED and AES studies. It was interfaced to conventional counting electronics and to a pulse height analyzer where  $N(E)$  spectra of the beta emission from  $^{14}\text{C}$  could be stored and integrated to obtain the total radioactivity present on the surface. The absolute detection efficiency (in the range 2.4–3.2%) was calibrated for the experimental counting geometry by depositing thin films of [ $^{14}\text{C}$ ]polymethylmethacrylate onto the single crystals and by monitoring the  $^{14}\text{C}$  count rate as a function of the amount deposited (15). Using this system  $^{14}\text{C}$ -containing species could be easily detected at surface concentrations of  $10^{12}$ – $10^{13}$  molec/cm $^2$ . Counting times were in the range of 3–10 min, and count rates

for adsorbed species and background were in the ranges 200–1600 and 2–5 counts per minute (cpm), respectively.

The (111) single crystal sample used in these investigations was deliberately cut very thin so that the polycrystalline edges would constitute less than about 15% of the total platinum surface area. The crystal was cleaned by repeated cycles of 1.0-keV Ar<sup>+</sup> bombardment at 1000 K, O<sub>2</sub>-treatment at 10<sup>-7</sup> Torr and 900–1200 K, and annealing to 1300 K. The crystal temperature was continuously regulated to  $\pm 2$  K with a precision temperature controller referenced to a Chromel–Alumel thermocouple spot-welded to the edge of the crystal. Heating rates in the range 12–90 K/sec were employed for all thermal desorption measurements.

Unlabeled hydrocarbon reagents were of the highest obtainable research purity. The liquid hydrocarbons were outgassed by repeated freeze-pumping cycles at 77 K prior to use. <sup>14</sup>C-labeled ethylene (Amersham, 128 mCi/mmol, radiochemical purity  $\geq 99.5\%$ ) was used as supplied after brief freeze pumping at 77 K.

## RESULTS AND DISCUSSION

### A. [<sup>14</sup>C]Ethylene Chemisorption and Dehydrogenation on Pt(111)

Isotherms obtained for [<sup>14</sup>C]ethylene chemisorption on Pt(111) at 330–570 K are shown in Fig. 2. For temperatures below about 450 K, the initial sticking coefficient  $S_0$  and the saturation coverage  $C_s$  were constant. At higher temperatures a second and slower adsorption process was apparent, which continued for exposures above 20 L (1 L = 10<sup>-6</sup> Torr · sec, uncorrected for ion gauge sensitivity). As demonstrated below, the slow adsorption process was accompanied by extensive dehydrogenation and rearrangement of the surface species.

Ethylene chemisorption on Pt(111) at 300–430 K leads to the formation of surface ethylidyne species which display a 2 × 2 overlayer structure. Dynamical LEED in-

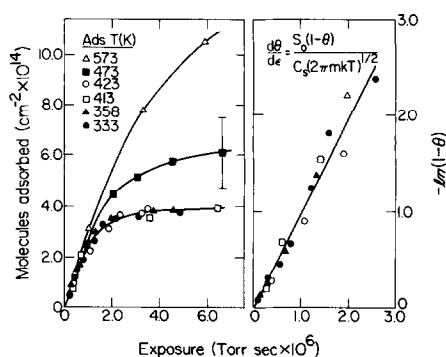


Fig. 2. Adsorption isotherms for [<sup>14</sup>C]C<sub>2</sub>H<sub>4</sub> chemisorption on Pt(111) at 330–570 K (left frame). The adsorption behavior at 330–420 K is well described by a first-order Langmuir model (right frame).

tensity analysis (3, 6), HREELS (3, 4), and TDS (4, 5) studies have revealed that they occupy threefold hollow adsorption sites with the C–C internuclear axis directed normal to the platinum surface and with C–C and Pt–C bond distances of 1.5 and 2.0 Å, respectively. The radiotracer uptake curve (Fig. 2) shows that this species forms according to first-order Langmuir kinetics, i.e.

$$\frac{d\theta}{d\varepsilon} = \frac{S_0}{C_s(2\pi mkT)^{1/2}} (1 - \theta), \quad (1)$$

where  $\varepsilon$  is the gas exposure,  $C_s$  is the ethylidyne saturation coverage ( $C_s = 3.8 \times 10^{14}$  molec/cm<sup>2</sup>), and  $S_0$  was constant at  $0.9 \pm 0.2$  over the temperature range 330–420 K.

Hydrogen thermal desorption spectra representing the sequential dehydrogenation of ethylene chemisorbed on Pt(111) at 110–570 K are shown in Fig. 3. As discussed in detail by Salmeron (5), ethylene dehydrogenation following adsorption at about 110 K is characterized by three sets of H<sub>2</sub>-desorption peaks. The initial C–H bond activation produces a sharp peak at 295 K which corresponds to ethylidyne formation. The second dehydrogenation reaction occurs at about 470 K and corresponds to the loss of two hydrogen atoms per ethylidyne (4, 5). A final dehydrogenation of the carbonaceous residue occurs at higher

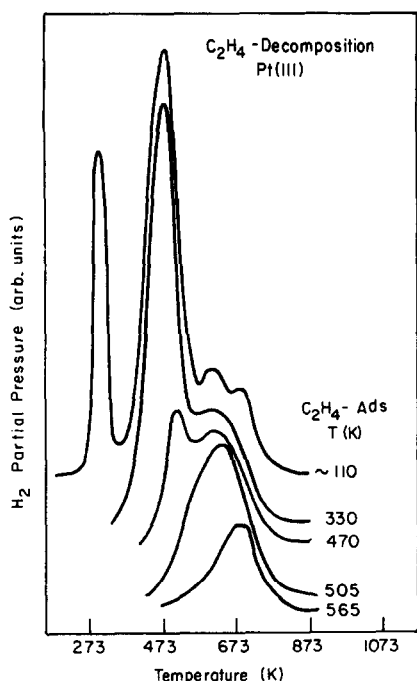


FIG. 3. Hydrogen thermal desorption spectra representing the sequential dehydrogenation of  $\text{C}_2\text{H}_4$  chemisorbed on Pt(111) at 110–565 K. The heating rate was 88 K/sec except for the top curve reproduced from Ref. (5) where it was 12 K/sec.

temperatures and leads to the formation of graphite on the surface.

Activation energies for the C–H bond breaking processes that produced the different hydrogen desorption peaks were estimated by assuming that all are unimolecular reactions. Kinetic analysis of the dehydrogenation steps is then identical to that for first-order molecular desorption which may be conveniently treated with the Redhead formula (16)

$$E_a = RT_p^2(\nu/\beta) \exp(-E_a/RT_p), \quad (2)$$

where  $\beta$  is the sample heating rate,  $\nu$  is surface reaction preexponential factor, and  $T_p$  is the temperature of the desorption peak maximum. The assumption of first-order reaction kinetics was justified by the fact that the desorption peak temperatures were invariant to changes in initial surface coverage. Assuming  $\nu = 10^{13} \text{ sec}^{-1}$ , the activation energies for ethylene dehydrogenation

were found to vary widely from about 18 kcal/mole for ethynylidyne formation to 35–43 kcal/mole for complete dehydrogenation.

The average (H/C) stoichiometry of the adsorbed species, expressed as hydrogen atoms per surface carbon atom, was determined as a function of adsorption temperature from the total areas under the hydrogen thermal desorption spectra. The desorption peak area was assumed to be proportional to the amount of hydrogen originally retained by the adsorbed species. Comparison of this peak area with the  $\text{C}_{273}/\text{Pt}_{237}$  AES peak-to-peak height ratio provided a measure of the initial (H/C) composition, as described in detail previously (13).

The composition of the strongly bound species resulting from ethylene chemisorption is temperature dependent in the 300–670 K range, as shown in Fig. 4. The hydrogen content of the surface species decreased with increasing adsorption temperature and approached zero at temperatures higher than 670 K.

### B. Reversibility of Sequential

#### Dehydrogenation: Radiotracer Studies of Ethylene Rehydrogenation and Hydrogen Transfer Reactions

Radiotracer decay curves representing

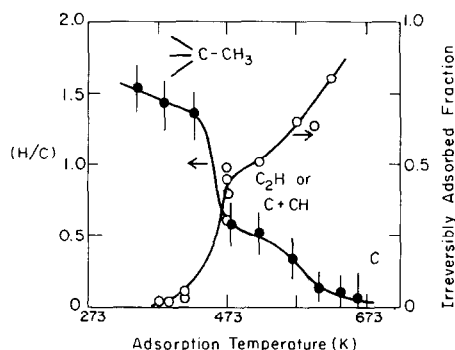


FIG. 4. Composition and reactivity of  $[^{14}\text{C}]$ ethylene chemisorbed on Pt(111) at 320–670 K. The irreversibly adsorbed fraction determined by radiotracer analysis displays an excellent correlation with the average hydrogen content (H/C) of the strongly bound surface species.

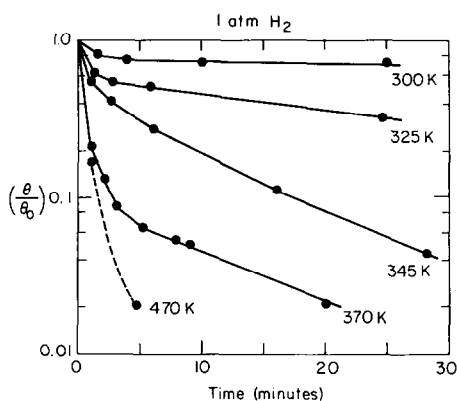


FIG. 5. Radiotracer decay curves illustrating the rehydrogenation of  $[^{14}\text{C}]$ ethylidyne species chemisorbed on Pt(111).

the rehydrogenation of ethylidyne chemisorbed on the (111) platinum surface are shown in Fig. 5. These species were prepared by chemisorbing  $[^{14}\text{C}]$ ethylene at 335–345 K and  $10^{-7}$  Torr using a constant exposure of 6 L. The rehydrogenation reactions were carried out at 300–470 K in the presence of 1 atm of flowing hydrogen. The reactions were interrupted at intervals of 1–10 min so that the residual coverage  $(\theta(t)/\theta(t=0) = \theta/\theta_0, \text{ in cpm/cpm}_0)$  of the radioactive surface species could be determined as a function of total reaction time. Two observations are significant: (1) the ethylidyne species became highly reactive only at temperatures higher than about 340 K, and (2) the rehydrogenation was not a first-order process. At 300 K only about 25% of the surface moieties were removed by rehydrogenation in 30 min of reaction time. By contrast, at 370 K or higher temperatures, the same surface species underwent essentially complete rehydrogenation in just 2–5 min. From the initial slopes of the decay curves the activation energy for ethylidyne hydrogenation can be very roughly estimated to be 5–10 kcal/mole.

These results are in excellent agreement with those obtained using HREELS, where the stability of ethylidyne was inferred from the observation that no changes occur in the vibrational spectra after 1 atm  $\text{H}_2$  exposure at temperatures up to about 330 K (8).

Hydrogenation of ethylene occurs readily under these conditions with turnover frequencies of 1–100 molecules/Pt  $\cdot$  sec (7), implying therefore that *hydrogenation reactions proceed in the presence of an ethylidyne saturated surface*.

A similar series of rehydrogenation reactions was carried out following the chemisorption of  $[^{14}\text{C}]$ ethylene on Pt(111) at 473 and 600 K. Ethylene adsorption at these temperatures produced surface species with average compositions " $\text{C}_2\text{H}$ " (473 K) and " $\text{C}$ " (600 K). Representative results are shown in Fig. 6. Rehydrogenation of these more strongly adsorbed species at 370–640 K proceeded in at least two distinct stages. A very rapid initial reaction which was complete within about 2 min was always followed by a very slow rehydrogenation process ( $R_h \leq 10^{-5}$  mole/Pt atom  $\cdot$  sec), which continued for hours without reaching completion. The rapid initial reaction appears to represent the hydrogenation of small C,  $\text{C}_2$ , CH, and/or  $\text{C}_2\text{H}$  fragments that are reportedly present following ethylene chemisorption at 470–650 K (4, 5). The second process, on the other hand, appears to represent the gasification of polymer carbon islands with very low hydrogen content. Similar catalytic behavior characterized by a two-stage rehydrogenation reaction was reported by Krebs and Bonzel (17) for the hydrogenation of surface carbon deposited on iron foils at 560 K.

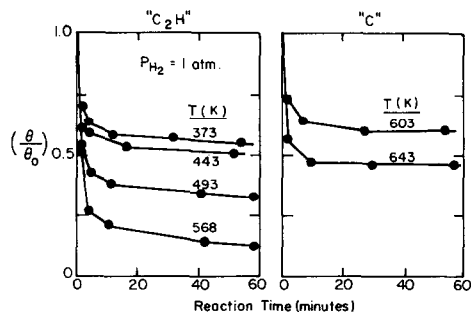


FIG. 6. Radiotracer decay curves illustrating the partial rehydrogenation of ethylene decomposition products with average composition " $\text{C}_2\text{H}$ " (left frame) and " $\text{C}$ " (right frame). These species were prepared by chemisorbing  $[^{14}\text{C}]\text{C}_2\text{H}_4$  on Pt(111) at 470 and 600 K.

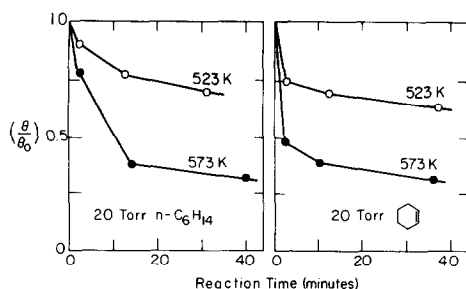


FIG. 7. Radiotracer decay curves illustrating hydrogen transfer reactions between n-hexane (left frame) or cyclohexene (right frame) with “ $\text{C}_2\text{H}$ ” surface species that were produced from  $^{14}\text{C}$  ethylene chemisorption on Pt(111) at 470 K.

These results show that for temperatures higher than about 470 K, ethylene chemisorption on Pt(111) is always partially irreversible. The proportion of the total surface carbon which exists in the inactive form increases with increasing adsorption temperature. In Fig. 4 the irreversibly adsorbed fraction is shown as a function of temperature along with the (H/C) stoichiometry of the adsorbed layer as determined from thermal desorption studies. The irreversibly adsorbed fraction was defined as the proportion of preadsorbed  $^{14}\text{C}$  ethylene which could not be removed by rehydrogenation (40–80 min reaction time) at the same temperature at which the initial adsorption was carried out. *The (H/C) ratio displayed a striking correlation with the adsorption reversibility.* Sequential dehydrogenation of ethynide to “ $\text{C}_2\text{H}$ ”-like species at 450–470 K was accompanied by a corresponding decrease in reversibility from 95–100% to about 50–70%. The reversibility approached zero as the hydrogen content decreased further at higher adsorption temperatures.

The fact that the amount of inactive carbon deposited at 473 K was dependent upon the temperature of subsequent rehydrogenation reactions suggests that the process that causes the formation of the inactive carbon involves two independent pathways. The initial formation of inactive carbon responsible for the overall shape of Fig. 6 appears to occur during adsorption. Further polymerization, which competes

with direct hydrogenation, appears to occur during the initial stages of the rehydrogenation reactions. Provided that the activation energy for inactive carbon formation is smaller than that for hydrogenation, the irreversibly adsorbed fraction should decrease with increasing reaction temperature as observed experimentally. Further studies are in progress to better clarify the inactive carbon formation process.

The formation of inactive metal–organic surface species derived from  $^{14}\text{C}$  ethylene on alumina-supported Ni (18), Pd (18), Rh (18, 19), Ir (20), and Pt (18) catalysts was previously investigated by Thomson and Webb and co-workers. Inactive carbonaceous species were detected under all conditions of direct hydrogenation and hydrogen transfer with unlabeled ethylene and acetylene at 290–470 K. At 290 K, the irreversibly adsorbed fraction decreased in the sequence Pd (63%) > Ni (20%) > Ir (6–13%) > Pt (4–7%). The inactive fraction retained by the platinum catalyst increased to 40–60% at 470 K. These results appear to be in excellent agreement with those reported here for the small area (111) platinum single crystal surface.

The strongly adsorbed “ $\text{C}_2\text{H}$ ” fragments resulting from  $^{14}\text{C}$  ethylene chemisorption on Pt(111) at 470 K were also active for intermolecular hydrogen transfer reactions with unlabeled hydrocarbons. Radiotracer decay curves illustrating hydrogen transfer between “ $\text{C}_2\text{H}$ ” and n-hexane or cyclohexene at 523–573 K are shown in Fig. 7. An interesting feature of the hydrogen transfer reactions is the ease with which they occurred. Initial disappearance rates for the active  $^{14}\text{C}$ -containing species by hydrogen transfer with 20 Torr of n-hexane or cyclohexene appear to be within an order of magnitude of those for direct hydrogenation in 1 atm of hydrogen. Hexenes and benzene were detected as by-products of the hydrogen transfer reactions. Cyclohexene (a good hydrogen donor) underwent hydrogen transfer to “ $\text{C}_2\text{H}$ ” more rapidly than n-hexane (a poor hydrogen donor). In the absence of hydrogen, the hydrogen transfer reactions were accompanied by the forma-

tion of high concentrations of carbonaceous deposit on the platinum surface ( $C_{273}/Pt_{237} = 5-8$ ), as measured by AES. The pathway by which hydrogen transfer takes place remains uncertain at this time. While a direct transfer mechanism cannot be ruled out, it appears more likely that this reaction is mediated by dehydrogenation of unlabeled hydrocarbon molecules on the metal surface followed by addition of chemisorbed hydrogen to the  $^{14}C$ -containing species.

It should be noted that neither hydrogenation nor hydrogen transfer could be detected at low reactant pressures ( $10^{-8}$ – $10^{-6}$  Torr). Weakly adsorbed species that can be produced at atmospheric pressures appears to be an essential requirement for activity in these chemical reactions.

The radiotracer studies clearly demonstrate that hydrogen transfer reactions take place readily between hydrocarbon species strongly chemisorbed on the (111) platinum single crystal surface. Previous studies of cyclohexene hydrogenation and disproportionation catalyzed at 425 K over Pt(322) revealed that direct hydrogenation was 10 times faster than hydrogen transfer (12, 20). Because the activation energy for disproportionation ( $\sim 16$  kcal/mole) was larger than that for direct hydrogenation (5–6 kcal/mole), the importance of the hydrogen transfer pathway is expected to increase with increasing reaction temperature.

The notion that hydrogen transfer reactions may be important in hydrocarbon catalysis is not new. Thomson and Webb (22) have argued that a hydrogen transfer mechanism provides a general explanation for the patterns of catalytic activity displayed by metal catalysts in olefin hydrogenation reactions. Gardner and Hansen (23) reached a similar conclusion in connection with studies of ethylene hydrogenation over tungsten catalysts. Our results (7) certainly tend to confirm that hydrogen transfer reactions are important. More detailed kinetic studies of the hydrogen transfer pathway would be very valuable to determine the relevance of these processes.

## ACKNOWLEDGMENTS

This work was supported by the Director, Office of Energy Research, Office of Basic Energy Sciences, Materials Sciences Division of the U.S. Department of Energy, under Contract DE-AC03-76SF00098. We are grateful to the Shell Development Company for supplying the [ $^{14}C$ ]ethylene.

## REFERENCES

1. Koestner, R. J., Van Hove, M. A., and Somorjai, G. A., *J. Phys. Chem.* **87**, 203 (1983).
2. Kesmodel, L. L., and Gates, J. A., *Surf. Sci.* **111**, L747 (1981).
3. Kesmodel, L. L., Dubois, L. H., and Somorjai, G. A., *J. Chem. Phys.* **70**, 2180 (1979).
4. Baro, A. M., and Ibach, H., *J. Chem. Phys.* **74**, 4194 (1981) and references therein.
5. Salmeron, M., and Somorjai, G. A., *J. Phys. Chem.* **86**, 341 (1982).
6. Koestner, R. J., Frost, J. C., Stair, P. C., Van Hove, M. A., and Somorjai, G. A., *Surf. Sci.* **116**, 85 (1982).
7. Zaera, F., and Somorjai, G. A., *J. Amer. Chem. Soc.* **106**, 2288 (1984).
8. Bent, B. E., Koel, B., Zaera, F., and Somorjai, G. A., in press.
9. Creighton, J. R., Ogle, K. M., and White, J. M., *Surf. Sci.* **138**, L137 (1984).
10. Schlatter, J. C., and Boudart, M., *J. Catal.* **24**, 482 (1972).
11. Bond, G. C., Phillipson, J. J., Wells, P. B., and Winterbottom, J. M., *Trans. Faraday Soc.* **60**, 1847 (1964).
12. Davis, S. M., and Somorjai, G. A., in *The Chemical Physics of Solid Surfaces and Heterogeneous Catalysis* (D. A. King and D. P. Woodruff, Eds.), Elsevier, Amsterdam, 1982.
13. Davis, S. M., Zaera, F., and Somorjai, G. A., *J. Catal.* **77**, 439 (1982).
14. Davis, S. M., Zaera, F., and Somorjai, G. A., *J. Catal.* **85**, 206 (1984).
15. Davis, S. M., Gordon, B. E., Press, M., and Somorjai, G. A., *J. Vac. Sci. Technol.* **19**, 231 (1981).
16. Redhead, P. A., *Vacuum* **12**, 203 (1962).
17. Krebs, H. J., and Bonzel, H. P., *Surf. Sci.* **99**, 570 (1980).
18. Taylor, G. F., Thomson, J. J., and Webb, G., *J. Catal.* **12**, 191 (1968).
19. Reid, J. U., Thomson, S. J., and Webb, G., *J. Catal.* **30**, 372 (1973).
20. Norval, S. V., Thomson, S. J., and Webb, G., *Appl. Surf. Sci.* **4**, 51 (1980).
21. Davis, S. M., Ph.D. thesis, University of California, Berkeley, 1981.
22. Thomson, S. J., and Webb, G., *J. Chem. Soc. Chem. Commun.*, 526 (1976).
23. Gardner, H. C., and Hansen, R. J., *J. Phys. Chem.* **74**, 3298 (1970).